Research Square

Preprints are preliminary reports that have not undergone peer review.
They should not be considered conclusive, used to inform clinical practice,
or referenced by the media as validated information.

Research on Fault Diagnosis and Control Strategies for Power Batteries

Zibo Ye
Guangdong Polytechnic Normal University
Qianqian Zhu
Guangzhou Tianshu Testing Technology Co., Ltd
Xingfeng Fu
fxf1000@163.com

GAC AION NEW ENERGY AUTOMOBILE CO., LTD
Guoxin He
GAC AION NEW ENERGY AUTOMOBILE CO., LTD

Article

Keywords: Battery fault diagnosis system, Insulation, Fuzzy theory, Fault identification

Posted Date: September 7th, 2026

DOI: https://doi.org/10.21203/rs.3.rs-10414631/v1

License: This work is licensed under a Creative Commons Attribution 4.0 International License.
Read Full License

Additional Declarations: No competing interests reported.

Version of Record: A version of this preprint was published at Scientific Reports on October 23rd, 2026.
See the published version at https://doi.org/10.1038/s41598-026-76291-5.

Research on Fault Diagnosis and Control Strategies for Power Batteries

Zibo Ye [1], Qianqian Zhu[2],Xingfeng Fu [3,*], Guoxin He[3]

[1] School of Automobile and Transportation Engineering, Guangdong Polytechnic Normal University, Guangzhou 510665, China.; e-mail: yezibo@gpnu.edu.cn

[2] Guangzhou Tianshu Testing Technology Co., Ltd,Guangzhou 511462, China.1421810519@qq.com

[3] GAC AION NEW ENERGY AUTOMOBILE CO., LTD. Guangzhou 511434, China. ; e-mail: fxf1000@163.com; heguoxin2004@163.com

* Correspondence: fxf3000@yeah.net ; Tel.: (0086-15818802380 initials)

Abstract: Vehicle electrification is a significant trend in the modern automotive industry. The battery pack is the most critical and sensitive component of an electric vehicle, necessitating precise and reliable designs to ensure safety. To achieve this, diagnosing and managing battery insulation and communication faults are proven methods that help identify issues and enhance product reliability. This paper presents the integration of fuzzy theory into the development of fault diagnosis systems for power battery systems, focusing on detecting unpredictable battery faults under various operational conditions and confirming actual faults. The study prioritizes identification accuracy while increasing iteration counts to further improve fault identification precision. Both simulated and empirical data indicate that the fuzzy theoretical model developed for diagnosing battery system faults achieves high accuracy in fault detection. Although the judgment time is slightly extended, it remains within acceptable design specifications. Multiple repeated experiments reveal that the judgment time of the designed BMS fuzzy diagnosis system has increased by approximately 4.6 seconds; however, the accuracy of insulation fault diagnosis has improved from 81.1% to 92.3%, and the accuracy of communication fault diagnosis has risen from 91.4% to 97.7%. Compared to similar studies, the accuracy of BMS fault diagnosis is notably high, and the fault handling measures effectively ensure overall vehicle safety.

Keywords: Battery fault diagnosis system, Insulation, Fuzzy theory, Fault identification.

1. Introduction

Power batteries serve as the pivotal components of electric vehicles (EVs), with their diagnostic and control technologies managed by battery management systems (BMS) and application technologies. A critical aspect of developing power battery systems is the ability to detect, identify, and assess battery faults in a timely and accurate manner. This capability significantly extends the lifespan of power batteries, enhances their consistency, and improves their reliability. However, the causes of faults in power batteries during operation can be complex and unpredictable, making it vital to avoid misjudgments that could compromise their normal functioning [1]. Therefore, achieving precise fault diagnosis in power batteries and preventing misjudgments are crucial for ensuring the safety and convenience of electric vehicle operation [2].

The operational environment of BMS is notably complex, characterized by various interference signals that can impede the accurate identification of battery faults. To effectively discern fault information, a high-precision computational model for power batteries has been developed using experimental data. The challenge posed by the limited availability of battery fault datasets is addressed through fault simulation. Subsequently, neural network algorithms are employed to analyze diverse battery fault data. By comparing these results with standard diagnostic models, methods to improve the precision and efficiency of BMS fault diagnosis are discovered. Insulation monitoring is a crucial technology for ensuring the personal safety [1]. J Yin developed an adaptive forgetting factor recursive least squares algorithm that employed fuzzy logic to adjust the forgetting factor in real-time. This approach effectively reduces system noise and battery voltage fluctuations, resulting in more accurate estimations and enhanced performance of the battery pack insulation detection system [3]. Typically, insulation resistance is defined as the resistance associated with the maximum leakage current when a power battery is short-circuited to the ground or the vehicle chassis. Z. Chen utilized a method that involved establishing an equivalent circuit model using a high-fidelity cell model and employing the recursive least squares method for model parameter identification, thereby improving system identification and state estimation for fault diagnosis. To monitor the insulation state between high voltage and ground in electric vehicles, a method was proposed that involved injecting a low-frequency signal into an additional loop to detect insulation

resistance values in real-time [4]. By periodically varying the resistance and voltage levels, the method's performance in detecting insulation faults under different electrical parameters was evaluated. The robustness of the algorithm in practical applications was validated through dynamic and static experiments, ensuring its effectiveness in real-time insulation detection [5].

Fluctuations in the State of Charge (SOC) can be correlated with insulation faults within the battery pack. Anomalies in insulation resistance may coincide with specific SOC levels, underscoring the importance of incorporating SOC data in fault diagnostics [6]. X. Hu [7] introduced the Fuzzy Adaptive Federated Filtering method for estimating the SOC of battery cells. This method integrates a fuzzy system to adapt to different SOC inconsistency distributions, thereby improving the accuracy of SOC estimation. While the local filter is employed to estimate the cell SOC, it may not adequately account for variations and inconsistencies among the battery cells, potentially leading to less accurate estimations compared to the fusion estimation algorithm. The fusion estimation algorithm is evaluated for its fault tolerance in the presence of measurement errors, demonstrating robustness in managing uncertainties and inaccuracies during the estimation process [7]. By integrating a difference state observer with fuzzy logic, this method calculates a self-discharge percentage factor, which is employed for continuous feedback correction of the hybrid battery pack's charge. The coefficients in this method can be adjusted at each full charge to prevent over-correction, thereby ensuring the stability and reliability of the SOC estimation process [8]. Nevertheless, real-world data for fault diagnosis often contains missing or inconsistent information, complicating accurate fault identification and diagnosis. Simulating real-world battery faults in a laboratory setting is challenging due to difficulties in replicating conditions such as varying temperatures, multiple load scenarios, and diverse charge-discharge cycles that contribute to faults [9]. Liu et al. [10] proposed a modified Shannon entropy-based method for diagnosing faults in battery systems of electric vehicles, which improved the accuracy of error judgment by analyzing the structural faults of the model to identify the causes of misdiagnosis. This approach aids in identifying cells with abnormal voltage fluctuations by sub-regioning the data and determining the probability of each region, achieving a significant reduction in the average relative misdiagnosis rate by 81.9%. Hong et al. [11] combined advanced entropy algorithms with statistical analysis and data-driven methods to develop a comprehensive approach to diagnosing faults in battery systems used in electric vehicles. However, the accuracy, generalizability, and robustness of the new entropy-based battery safety control strategy have yet to be verified and need confirmation in subsequent research. Kang et al. [12] designed an online fault diagnosis method to improve the accuracy of battery fault diagnosis by integrating measurement circuits and improving composite models. A novel Linear Regression Long Short-Term Memory (LRLSTM) based joint prediction strategy, which combined LSTM with multiple linear regression algorithms, was introduced for multi-forward-step prediction, allowing it to forecast SOC over multiple future time intervals [13]. Battery anomalies or faults caused by SOC irregularities (such as low SOC, SOC jumping, etc.) can be diagnosed in advance, helping to prevent more serious battery issues, including battery thermal runaway. This capability is particularly beneficial for real-time applications in electric vehicles, addressing concerns related to drivers' mileage anxiety. Currently, significant research advancements have been made in this area. These analytical methods have developed increasingly complex battery calculation models, integrating battery circuit synthesis to assess battery fault diagnosis status and improve diagnostic accuracy. All of these efforts have expanded the battery fault information sample database, incorporated additional sensors and detection devices, and increased the complexity of detection circuits and experimental databases, which in turn has raised design costs. Therefore, this manuscript aims to improve the accuracy of battery fault diagnosis while managing design expenses. Based on existing research findings, employing fuzzy theory to enhance the accuracy of battery fault diagnosis is a widely accepted and practical approach. Consequently, this paper endeavors to develop a battery fault diagnosis system grounded in fuzzy theory.

Y. Zheng integrated fuzzy logic into a data-driven method to optimize estimation results and controlled noise in the Kalman filter algorithm, thereby enhancing the accuracy of capacity and internal resistance estimations. The fuzzy system within this data-driven method processes variables such as current and temperature changes to the estimate internal resistance of electric vehicle batteries. By applying fuzzy rules, it establishes the relationship between these variables, resulting in more precise estimations [14]. The integration of fuzzy system reasoning with the data-driven method enhances the prediction accuracy of thermal runaway propagation several steps ahead. The

fuzzy system calculates the probability of thermal runaway in the battery, taking into account factors such as temperature, SOC, and heat transfer characteristics. Its optimization via the sparrow search algorithm further refines these predictions, as evidenced by a high coefficient of determination in experimental validations [15]. Tang X. et al. applied the state representation methodology (SRM) for battery fault diagnosis [16]. This approach utilizes normalized cell voltages instead of the original voltages, enabling the detection of subtle changes in the battery's state and facilitating quicker identification of faults. The fault detection time achieved through the SRM is compared with the alarm time of the actual vehicle's BMS. This comparison demonstrates that the proposed method can detect faults earlier than the BMS alarms, highlighting its practical advantages. However, the fixed reasoning structure inherent in many data-driven techniques hampers their ability to adapt to changes in electro-chemical properties of batteries during electric vehicle operations. Traditional data-driven methods often struggle with parameter settings and adjusting to time-varying conditions, which impedes accurate predictions. These limitations restrict the effectiveness of data-driven approaches in dynamic environments such as EVs.

Communication faults in BMS can arise from various sources, including offset, stuck, delay, and replay issues due to communication failures in the network layer [17]. These faults can compromise the reliability of battery sensor data, leading to safety and performance concerns within the BMS module. T. Kim et al. [18] utilized Artificial Intelligence-based methods, such as Convolution Neural Network (CNN), to improve the safety and reliability of battery energy storage systems by accurately identifying and addressing communication faults that might result from sensor data manipulation, cyber-attacks, or hardware malfunctions. Three types of battery sensor data - voltage, current, and SOC - are directly utilized as input for the CNN-based false data diagnosis model. The proposed CNN-based False Battery Data Detection and Classification model is validated through both simulation and experimental studies. Continuous monitoring of sensor data and communication channels is essential for the prompt detection and resolution of any faults, thereby enhancing the safety and reliability of the BMS. V.S.R. Kosuru [19] introduced an incipient bat-optimized deep residual network for the identification and classification of false battery data, further improving the safety and dependability of the BMS. However, this approach may not thoroughly address the potential trade-offs between system performance, computational efficiency, and real-time responsiveness. Additionally, it lacks a detailed comparison with other feature extraction methods or fault detection algorithms commonly used in BMS applications, which limits a comprehensive evaluation of the proposed system.

Due to the uncertainty in communication and insulation faults in power batteries, fuzzy theory is more appropriately applied to establish a specific fuzzy relationship among various faults. By continuously adjusting and correcting different weighting coefficients and membership relationships, the fault diagnosis strategy of the BMS develops a certain degree of fuzzy self-learning capability. Among the numerous factors influencing power battery faults, the key ones can be precisely identified. Thus, the impact of these comprehensive factors on battery faults can be expressed through functional relationships, allowing for the accurate identification of the root causes of faults. This enables prompt corresponding measures, thereby ensuring the safety of power battery usage.

Owing to the lack of certainty in the operational characteristics of power batteries, a multitude of random situations have arisen. Nevertheless, the expert database generated from statistical analysis still, to some extent, mirrors the fault characteristics and relevant influencing factors of power batteries during operation. By applying fuzzy theory to establish connections between these relevant influencing factors and fault characteristics, the fault diagnosis strategy can more rapidly identify the root cause of the issue. Through fuzzy self-learning, effective measures can be implemented to mitigate or eliminate the fault. This not only accelerates the diagnosis speed but also enables more prompt intervention in the fault handling process. Such an approach is advantageous for controlling further deterioration and development of faults, thus holding great practical value. Both domestic and international research has confirmed that the incorporation of expert databases for diagnostic self-learning substantially enhances the accuracy of battery fault diagnosis. Moreover, the system's ability to resist external interference and its overall robustness are also remarkably improved.

The novelty of this article lies in the establishment of a corresponding fuzzy relationship matrix database. This is based on experimental statistics of power battery fault data and the probability of fault occurrence during the operation of electric vehicles. Battery faults are characterized by

corresponding membership relationships and fuzzy vectors, which are defined according to their severity and frequency of occurrence. These fuzzy vectors are then associated with the relevant fault-handling measures. In line with the UDS diagnostic communication protocol specifications, appropriate protection measures and handling strategies are developed. As a result, the accuracy of fault diagnosis for electric vehicle power batteries is notably enhanced, and the time required for fault diagnosis and maintenance is considerably reduced.

The remainder of this paper is structured as follows. In Section 2, the development of diagnostic functions for the BMS is presented. This includes the diagnostic service testing process and the fault diagnostic calculation process. Section 3 focuses on the introduction of the fuzzy fault diagnosis system. Considering the changing driving conditions, the vehicle controller's fault diagnosis process consists of the fault detection module, the fault management information module, and the fault resolution module. Section 4 details the identification and simulation of battery insulation faults and battery communication faults. The results show that the simulation outcomes are in line with the design requirements. Section 5 elaborates on the insulation and communication fault tests carried out using electric vehicles (EVs). The fuzzy theoretical model developed for diagnosing battery system faults has demonstrated high accuracy in fault detection. Finally, Section 6 provides a summary, along with several concluding remarks and an outlook on future directions.

Abbreviations

KWP	Keyword Protocol 2000	CAN	Controller Area Network
EDU	Electronic Drive Control unit	HCU	Hybrid Control Unit
EDS	Electric Drive System	OSI	Open System Interconnect
VCU	Vehicle Control Unit	UDS	Unified Diagnostic Services
HIL	Hardware-In-the-Loop	HVIL	High Voltage Interlock
ECU	Electric Control Unit	DTC	Diagnostic Trouble Code
DID	Diagnostic Information Diagnostic	DEM	Diagnostic Event Manager
VIN	Vehicle Identification Number	FRM	Footstep Space Module
GPU	Graphics Processing Unit	FPGA	Field Programmable Gate Array

ECU [23]. Typically, a diagnostic tool sends a request to which the ECU responds. A fault code, which is utilized to identify ECU faults according to specific criteria, is stored in the ECU's non-volatile memory. Diagnostic data, accessible by diagnostic tools, includes: current data reflecting the ECU's operational state, such as vehicle speed, throttle opening and engine speed; stored data, which is ECU memory data recorded at specific moments, such as DTC; and static data, which includes constant internal ECU information, such as VIN codes [24].

The development phase of BMS fault diagnosis software encompasses the creation of fault detection functions within the TargetLink model, fault response and processing functions also within the TargetLink model, DTC storage functions in C code, and diagnostic service functions related to faults in C code. Additionally, it includes the integration of software from UDS protocol stack code to the application layer C code and the TargetLink model in C code [25]. This process is illustrated in Fig. 1.

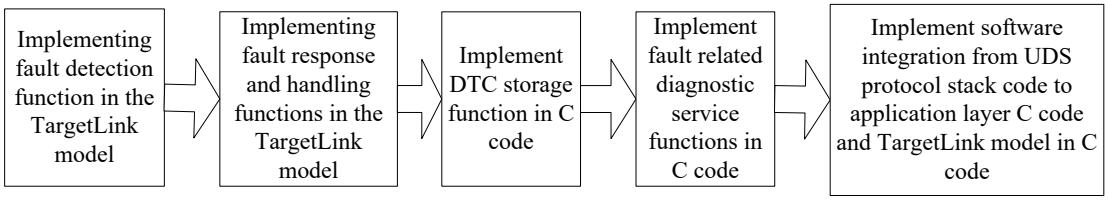


Fig. 1 BMS software fault diagnosis design and development process

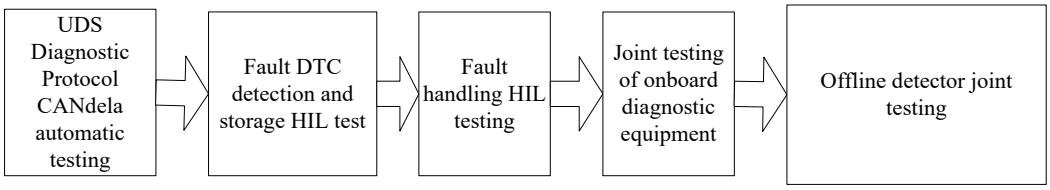


Fig. 2 Diagnostic service testing process

Fig. 2 presents the diagnostic service testing process. The objective of the testing and verification phase is to ensure that the software implementation of the BMS system's fault diagnosis strategy complies with the specifications of the UDS protocol. This phase encompasses a variety of tests, including automatic UDS protocol CAN delta testing, HIL testing for fault DTC detection and storage, fault response HIL testing, cooperative tests with onboard diagnostic tools, and tests conducted with offline diagnostic equipment.

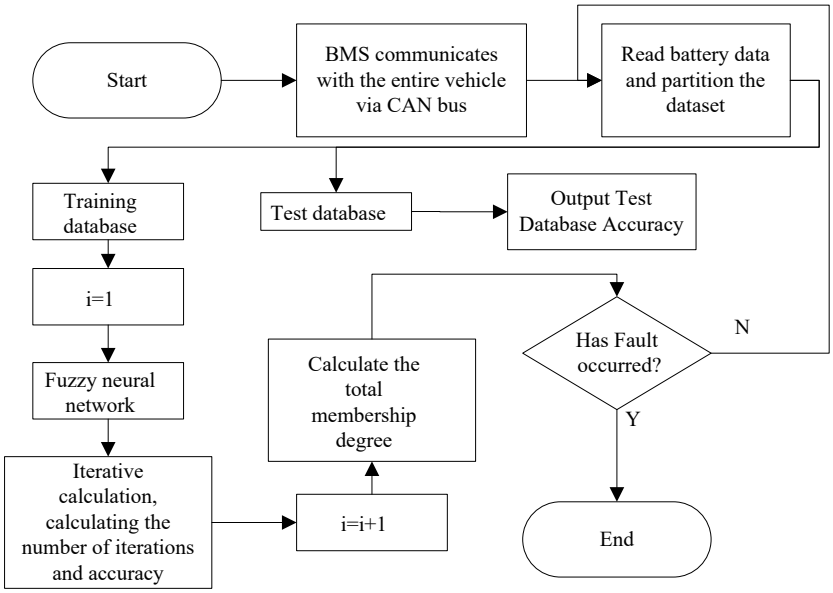


Fig. 3 Fault diagnostic calculation process

Fig. 3 illustrates the flowchart of the reasoning process for the fuzzy theory expert system. Upon receiving a range of BMS signals, this expert system generates a fuzzy vector set that represents potential fault causes. It then applies various fault control thresholds to identify battery faults, fine-tuning these thresholds through experimental adjustments. The diagnostic procedure relies on forward inference, where the inference mechanism instantly accesses battery status data from a global database. The rule library's battery membership function calculates the degrees of membership for the battery status data. Finally, the fuzzy expert system makes threshold determinations to confirm the specific battery fault and initiates appropriate corrective actions.

3. A Fuzzy System Based Algorithm Model for Battery Fault Diagnosis

The electrochemical model for lithium-ion batteries (LIBs) is formulated through electrochemical equations that encapsulate the characteristics of these batteries by thoroughly analyzing their internal mechanisms, materials, spectral properties, and internal diffusion effects [26,27,28,29]. This research is targeted at developing a theoretical calculation model for power batteries. The results obtained from the model must be compared with the measured values recorded during vehicle operation. The model should be continuously refined to ensure that it aligns closely with the actual measurement results. By establishing fuzzy diagnostic data and correlation relationships, the subsequent trends and patterns of change can be predicted, which aids in fault diagnosis and assessment, thereby enhancing diagnostic accuracy and reducing the time required for diagnosis. In the subsequent theoretical calculation model for batteries, system process noise

and observation noise are incorporated to enhance the model's compliance with practical application scenarios.

$$\begin{cases} U_L = U_{OC}(SOC) - i(t)R_O - U_P \\ dU_P/dt = -U_P/R_P C_P + i/C_P \end{cases} \quad (1)$$

$$U_{Pb} = \int i dt + U_{Pb0} \quad (2)$$

Within this model, U_L denotes the terminal voltage, U_{OC} stands for the open-circuit voltage, $i(t)$ signifies the load current, R_O is the ohmic internal resistance, C_P is the electrode plate's equivalent capacitance, and U_P is the terminal voltage across the polarization capacitor C_P. The symbol i is used for current, C_b for the equivalent capacitance that depicts changes in the open-circuit voltage, and U_{Pb} for the terminal voltage across the capacitor C_b.

$$\begin{cases} \begin{bmatrix} SOC_k \\ U_{p,k} \end{bmatrix} = \begin{bmatrix} 1 & 0 \\ 0 & e^{-\Delta t/\tau} \end{bmatrix} \begin{bmatrix} SOC_{k-1} \\ U_{p,k-1} \end{bmatrix} + \begin{bmatrix} -\eta \frac{\Delta t}{C_{max}} \\ R_p\left(1-e^{-\Delta t/\tau}\right) \end{bmatrix} i_k + w \\ U_{L,k} = U_{oc}(SOC_k) - U_{p,k} - i_k R_o + v \end{cases} \quad (3)$$

Within the equation, C_{max} denotes the battery's maximum utilizable capacity, η represents the coulombic efficiency, Δt indicates the sampling interval, τ is the time constant, w signifies the process noise, and v refers to the observation noise.

In the correction algorithm for SOC and battery terminal voltage, the process noise w represents the correction amount derived from the calculation error of the battery model and the inaccurate input current value. On the other hand, the observation noise v is the correction value resulting from the measurement error of the battery terminal voltage. During actual operation, both the system process noise and the observation noise continuously vary over time. If these noise errors are not corrected promptly, they may negatively impact the final estimation result. To mitigate the interference caused by system noise errors, an adaptive matching module based on fuzzy theory is incorporated into the SOC algorithm. This module facilitates the timely correction of both the system's process noise and observation noise.

$$\mathrm{SOC}(k+1) = \mathrm{SOC}(k) - {\eta_i \Delta t i(k)}/{\eta_T}\,(1-\eta_n)C_n \quad (4)$$

$$Q_k = p(k-k') + \frac{1}{3}\sum_{n=k-2}^{k} \Delta x_k (\Delta x_k)^T \quad (5)$$

$$R_k = \frac{1}{3}\sum_{n=k-2}^{k} \Delta y_k (\Delta y_k)^T - C_k p'_k C_k^T \quad (6)$$

Additionally, in this formula, $\mathrm{SOC}(k+1)$ indicates the battery's State of Charge (SOC) at the moment $k+1$; $i(k)$ denotes the current value for the interval $k \sim k+1$; Q_n is the battery's rated capacity. The correction coefficients for the charge-discharge ratio, temperature, and number of charge-discharge cycles on battery capacity, represented as η_i, η_T and η_n, respectively, are determined through analysis of battery charge-discharge experimental data [30].

In the fuzzy adaptive calculation module for noise error, $\mathrm{x_k}$ represents the system state variable at time k, while $\Delta\mathrm{x_k}$ is defined as the deviation between the true value and the estimated value of the system state variable at time k. To obtain formula (5), a weighted average operation is applied to the errors between the true and estimated values of the system state variables during the first three time steps. Following this, the differences between the true and estimated values within the error matrix of these state variables are summed up.

Let $\Delta\mathrm{y_k}$ denotes the deviation between the true and estimated values of the observed variable with respect to the state variable at time k. In a parallel manner, to obtain formula (6), the weighted average of the differences between the true and estimated values of the observed variable is first calculated over the first three time steps. Then, the input error generated by the variance error of the state variable is subtracted.

In the scope of this study, once the error value exceeds 30%, the correction calculation will be launched. The calculation model formula is revised as presented in formula (7). The correction calculation of the State of Charge (SOC) is based on the fuzzy relationship matrix. It is adjusted and corrected in accordance with the distinct weighted values in the calculated results and the Open

Circuit Voltage - State of Charge (OCV-SOC) table retrieved from the lookup table. It should be noted that the proportion of these weighted values will change according to the working state and the working environment.

$$\begin{cases} \begin{bmatrix} \dot{U}_b \\ \dot{U}_p \end{bmatrix} = \begin{pmatrix} 0 & 0 \\ 0 & -1/C_pR_p \end{pmatrix} \begin{bmatrix} U_b \\ U_p \end{bmatrix} + \begin{bmatrix} 1/C_b \\ 1/C_p \end{bmatrix} I_L \\ [U_L] = [-1 \quad -1] \begin{bmatrix} U_b \\ U_p \end{bmatrix} + [-R_O][I_L] + [U_{OC}] \end{cases} \tag{7}$$

In the described model, the voltages U_b and U_p correspond to the state variables of two capacitors, while the terminal voltage U_L of the battery is considered the output variable.

Eq.1-Eq.5 are relationship models established based on battery experimental data for voltage, SOC, and current. They can simulate and calculate the changes in voltage, current, temperature, and internal resistance under different operating conditions. These simulation results and change curves can be used as input variables for the fuzzy diagnosis system. The fuzzy diagnosis system comprehensively compares and judge whether there is a fault based on the calculation results of the model and the input of various working condition signals, determining the possible fault level. It reminds VCU to take different treatment measures according to different fault levels and sends diagnostic processing information to the instrument panel to remind drivers and passengers to handle it.

Fuzzy neural networks are characterized by their use of fuzzy weight coefficients or inputs. These networks, whether functioning as approximators or as pattern storage systems, require the learning and optimization of weight coefficients. The key to optimizing these coefficients in fuzzy neural networks lies in the learning algorithms employed. For logical fuzzy neural networks, error-based or supervised learning algorithms are applicable. Arithmetic fuzzy neural networks may utilize algorithms such as the fuzzy backpropagation (BP) algorithm or genetic algorithms. Presently, an effective algorithm for hybrid fuzzy neural networks has not been established. Nonetheless, hybrid fuzzy neural networks are predominantly utilized for computation rather than learning, which eliminates the necessity for a learning process [31,32].

Fuzzy control, an application of fuzzy theory, has effectively addressed challenges that traditional control theory encounters across various domains, yielding persuasive outcomes. This approach encapsulates control strategies from human experts for specific targets or processes into a collection of control rules framed as "IF (condition) THEN (action)." Through fuzzy reasoning, a set of control actions is derived and implemented on the target or process, forming a series of conditional statements. Both the state and control actions are expressed as quantified fuzzy linguistic sets [33].

The performance and outcomes of an algorithm are intricately linked to the diversity, convergence, and iteration count of the sample population. Consequently, the number of iterations and convergence metrics are incorporated as inputs to the fuzzy system, with crossover and mutation probabilities dynamically adjusted throughout the iteration process. Fig. 4 illustrates the relationships of fuzzy functions. To quantify the algorithm's iterations, iteration values are confined to the range [0, 1], and the spread of the convergence metric is normalized. Inputs from each sample are categorized into three triangular membership functions (denoting the input value's magnitude as low, mid, and high). Meanwhile, outputs are divided into five triangular membership functions (representing the output value's magnitude as low, mid-low, mid, mid-high, and high).

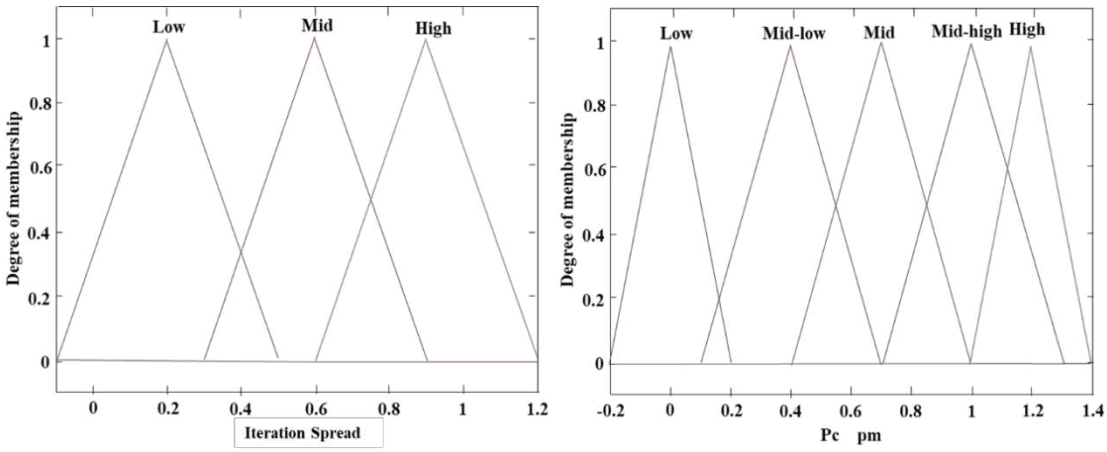


Fig. 4 The relationships of fuzzy functions

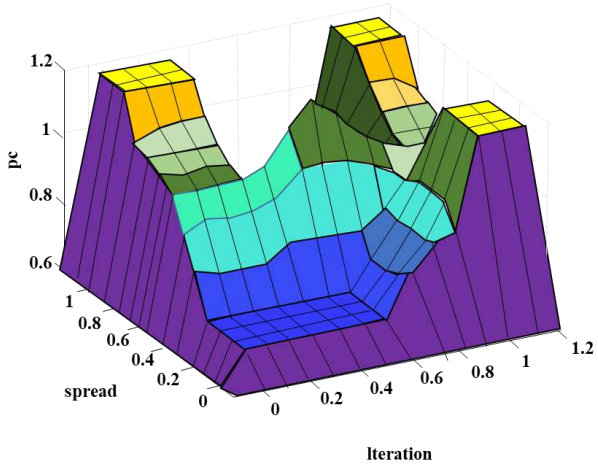


Fig.5 Fuzzy system output diagram of cross probability

Fig. 5 presents the output results of the fuzzy system concerning cross probability. The fault data from the defective battery is calculated using their respective fault membership functions to derive membership values. Based on the established correlation between the experimental fault data and the fault levels, this information is input into the fuzzy judgment system library, which is constructed using fuzzy rules, to diagnose the relevant fault information and determine appropriate corrective measures. During the training and calculation process of the fuzzy fault diagnosis system, the newrb function in Matlab software is employed. The key constant for training is the radial grassroots dispersion function spread, which represents the expansion speed set to 1. Additionally, the mean square error accuracy is configured to 0.001.

The fault handling mechanism for specific faults is generally categorized into three fault detection, fault management, and system fault response and resolution [34]. Fig. 6 presents a flowchart for fault diagnosis and assessment utilizing fuzzy theory. The vehicle controller's fault diagnosis process encompasses these three main stages: fault detection, fault management, and fault resolution. The process begins with fault detection at the VCU's input/output interface and through its functional definition to identify specific VCU faults. Identified faults are then automatically logged in the system's lower layer with predetermined fault codes and frozen frames. Ultimately, distinct faults are directly linked to their respective fault resolution actions, prompting each functional module to implement designated failure protection protocols.

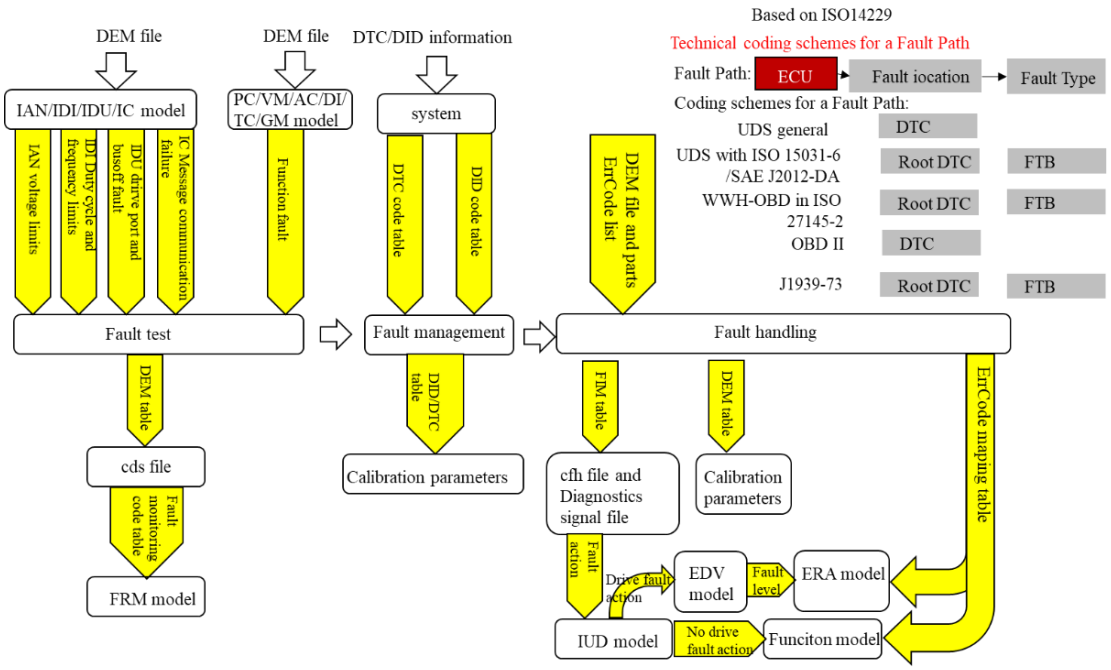


Fig. 6 Fault handling flowchart based on Fuzzy System

As depicted in Fig. 6, when various fault signals are received, the processor evaluates and processes these signals within the fault detection module. It generates related menu files and predicts subsequent fault management steps by comparing relevant fault code data using the FRM model. Within the fault management information module, fault severity levels and anticipated responses are determined based on judgment logic and calibration parameters derived from the DTC and DID lists. In the fault resolution module, a comprehensive evaluation of the driver's actions and the vehicle's condition, informed by the fault management data and severity levels, guides the selection of appropriate fault responses tailored to different types of information. This thorough fault diagnosis and resolution cycle is iteratively refined and validated in response to changing driving conditions.

4. Identification and execution measures of Battery Faults

Drawing upon the theoretical analysis from the previous section and in accordance with the design requirements of the UDS diagnostic protocol, a BMS fault diagnosis strategy based on fuzzy theory has been developed. This development involves the construction of a related expert library and the establishment of connection relationships grounded in fuzzy theory. Among the various types of battery faults, typical insulation faults and communication faults have been deliberately selected as examples for focused analysis. The objective of this analysis is to assess whether the design outcomes of creating a power battery fault diagnosis system using fuzzy theory meet the specified design requirements.

4.1 Typical fault control threshold information and execution measures for batteries

Signals and communication data from electric vehicles are frequently contaminated with a considerable amount of erroneous noise. To minimize false alarms and enhance detection accuracy, it is essential to develop specific criteria for assessing the actual occurrence of faults. This research utilizes CAN communication signals and sensor fault data as inputs for the fuzzy system. Thresholds for estimation are established to scrutinize and evaluate the fault data, ultimately determining the presence of faults. Only with such confirmation can appropriate fault resolution measures be implemented [35,36,37].

Upon detecting a fault, the BMS initiates a designated debounce process. Both fault confirmation and fault recovery must adhere to a calibrated debounce time. The debounce module functions as a timer that begins when the enable signal MonEna set to 1, and the program has the ability to reset it. After a reset or initialization, the countdown is reverted to 0 [38].

If the monitoring result MonDfct of the fault detection report is 1, it indicates that a fault has occurred, and the "fail" timer increases. Once this timer reaches the calibratable threshold for "fail" (tiDfct), bits 0, 1, and 3 of the status word stDbc are set to 1.

If the monitoring result MonDfct of the fault detection report is 0, indicating that no fault has occurred, the "pass" timer increases. When this timer reaches the calibrated threshold (tiOk) for "pass", bit 0 of the status word stDbc is reset to 0.

The anti-shake debounce module of the HCU operates according to specific rules: it is constructed around a counter that increments when the reported fault monitoring result MonOk is 1. Conversely, if the reported fault monitoring result is 0, indicating no fault detection, the counter decrements.

This software architecture ensures that "pass" and "fail" detections cannot occur simultaneously. The analysis focuses on two specific fault types within BMS fault diagnosis design: battery insulation faults and internal communication faults. These examples illustrate the diagnostic system's design approach. Insulation faults are chosen for their distinctiveness and representativeness in BMS fault diagnosis system design. Moreover, the diagnosis and remediation of internal communication faults in BMS exhibit unique design features compared to other components of electric vehicles. The data in the software model design library is compiled from a substantial amount of experimental battery data, and the control thresholds presented in the table also have been measured.

Tab. 1. Battery insulation failure threshold table

Item	Fault name	Fault threshold	Fault tolerance time	Diagnostic start conditions	Diagnostic cycle/Recovery time	Fault recovery value	vehicle operation		External charging	Vehicle standing still	
							Discharge	Charge		Discharge	Charge
Insulation	AC insulation	≤1000Ω/V	20s	From initialization to high voltage power down	10ms/20s	≥1250 Ω/V	/	/	enable	enable	enable
		≤750Ω/V	20s		10ms/20s	≥1000 Ω/V	/	/	enable	enable	enable
		≤300Ω/V	20s		10ms/20s	≥550Ω/V	/	/	Stop	Stop	Stop
	DC insulation(closed relay)	≤1000Ω/V	20s		10ms/20s	≥1250 Ω/V	Map	Map	/	enable	enable
		≤750Ω/V	20s		10ms/20s	≥1000 Ω/V	10kW	10kW	/	enable	enable
		≤500Ω/V	20s		10ms/20s	≥750Ω/V	Request to power down		/	Stop	Stop
	DC insulation(open relay)	≤1000Ω/V	20s	From initialization to low voltage power down	10ms/20s	≥1250 Ω/V	Map	Map	/	enable	enable
		≤750Ω/V	20s		10ms/20s	≥1000 Ω/V	10kW	10kW	/	enable	enable
		≤500Ω/V	20s		10ms/20s	≥750Ω/V	Request to power down		/	Stop	Stop

Table 1 presents a threshold chart for diagnosing power battery faults, which, when combined with relevant auxiliary signals, facilitates fault identification. For instance, in diagnosing insulation faults, the BMS must detect a signal indicating low insulation resistance 20 consecutive times, along with other auxiliary judgment data, to definitively identify an insulation fault and initiate the appropriate response actions. Specifically, an insulation resistance value of ≤ 1000 Ω/V indicates a minor level one insulation fault, allowing normal vehicle operation without changes to the charging and discharging power maps. If the insulation resistance value reaches ≥ 1250 Ω/V, the fault self-corrects. Conversely, an insulation resistance value of ≤ 750 Ω/V triggers a report of a secondary insulation fault, restricting battery discharge and feedback power to 10 kW and placing the vehicle in a reduced operational state with significantly lowered charging and discharging power. This fault self-corrects when the insulation resistance value reaches ≥ 1000 Ω/V. However, an insulation resistance value of ≤ 500 Ω/V indicates a severe level three insulation fault, leading to a complete operational halt and a request from the BMS to power off the vehicle, which self-corrects when the insulation resistance value is ≥ 750 Ω/V.

Table 2 details the control thresholds and response protocols for BMS CAN communication faults, outlining fault recovery conditions and post-fault action plans. Communication faults are categorized into internal BMS communication faults, external communication faults, and charging communication faults, each with distinct operational environments and specific protective measures and judgment criteria. For internal communication issues, various diagnostic and control strategies are employed based on the specific scenario. Upon detecting an internal communication fault, the

BMS gathers additional auxiliary signals for fault analysis and decision-making. If the charging gun connection status is 1, indicating a successful connection, the vehicle should remain stationary while charging. During an internal communication fault, neither charging nor discharging of the power battery is permitted. If the power battery cannot be charged, the vehicle becomes immobilized. In the event of a communication failure within the battery and the disconnection of the charging gun, the vehicle's diagnostic system determines that charging should not occur, thereby restricting charging while allowing limited discharging. This enables the vehicle to move slowly and safely, facilitating self-rescue while ensuring the safety of the driver and passengers.

Tab. 2. Battery CAN communication failure threshold table

Fault name	Fault threshold	Fault tolerance time	Diagnostic start conditions	Diagnostic cycle/Recovery time	Fault recovery value	Fault recovery value	vehicle operation		Vehicle standing still	
							Discharge	Charge	Discharge	Charge
Internal SCAN communication failure	**/**	**2s**	**Initialize to lower low voltage**	**10ms/immediately**	**Fault clearing**	**Communication message recovery**	**10kW**	**10kW**	**enable**	**Stop**
VCU message loss	**/**	**2s**	**Initialize to lower low voltage**	**10ms/immediately**	**Fault clearing**	**Communication message recovery**	**10kW**	**10kW**	**enable**	**Stop**
OBC message loss	**/**	**2s**	**Initialize to lower low voltage**	**10ms/immediately**	**Fault clearing**	**Communication message recovery**	**/**	**/**	**Stop**	**enable**
EVCAN message loss	**Error Count > 255**	**/**	**Initialize to lower low voltage**	**10ms/immediately**	**Fault clearing**	**Communication message recovery**	**Request to power down**		**Stop**	**Stop**
DCCAN busoff (CHCAN)	**Error Count > 255**	**/**	**Initialize to lower low voltage**	**10ms/-**	**Power off clearing**	**Fault clearing**	**Request to power down**		**Stop**	**Stop**
EcCAN busoff(SCAN)	**Error Count > 255**	**/**	**Initialize to lower low voltage**	**10ms/-**	**Power off clearing**	**Fault clearing**	**Request to power down**		**Stop**	**Stop**

4.2 Identification and simulation of battery insulation faults

Fig. 7 illustrates the insulation simulation model of the high-voltage battery segment within the power battery's high-voltage circuitry, developed using Simulink software. In this model, the BMS is activated to initiate the power-on sequence. Upon activation, a 100 kΩ resistor is introduced at the 3-second mark to evaluate the efficiency of the insulation detection system in identifying insulation faults within the battery pack. This also assesses whether the implemented fault management logic aligns with the established fault control thresholds and if the actuator's response sequence complies with the predefined fault management protocol. Additionally, it examines whether the timing of fault detection and response adheres to the design specifications.

In EV, the insulation detection function for the alternating current (AC) circuit is managed by the insulation protection system (IPS), while the BMS is solely responsible for insulation detection in the high-voltage direct current (DC) circuit. Consequently, the insulation detection of AC circuits is not covered in what we've been working on. As a result, the fuzzy fault diagnosis system that we developed here doesn't integrate the AC insulation fault detection. Still, in terms of the development and design of the fuzzy fault diagnosis system, the input and output variables linked to AC insulation faults and the fuzzy rules for evaluation are of a similar nature.

Fig. 8 displays the outcomes derived from the simulation. The results indicate that after the BMS starts up and successfully completes its self-check, achieving a BMS state value of 2 (which signifies that the main relay is closed), the BMS transitions into an operational state. At the calibration point, 3 seconds into the simulation, a resistor with a series resistance of 100 kΩ is introduced. Approximately 3 seconds later, the BMS detects an insulation fault and signals this fault condition. Within a interval span of about 150 ms, the BMS communicates the fault, promptly adjusting the BMS state value to 9 (indicating that the power hold relay is open). Following an additional verification period of approximately 100 ms, the BMS again flags an insulation fault, with the findings of the entire simulation aligning with the design parameters outlined in the control

threshold table. The response duration meets the design expectations. Thus, the simulation demonstrates that with the integration of appropriate series resistors, the BMS is capable of providing accurate fault diagnoses and executing the necessary corrective actions.

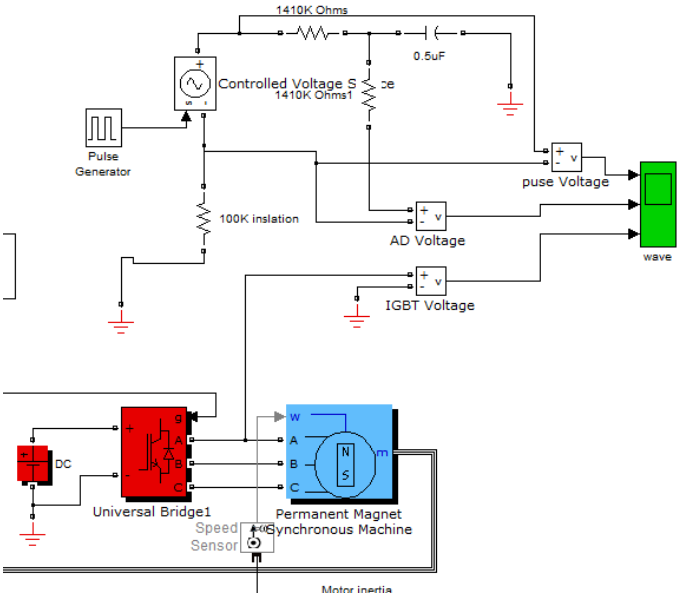


Fig. 7 Insulation resistance simulation circuit diagram (DC side)

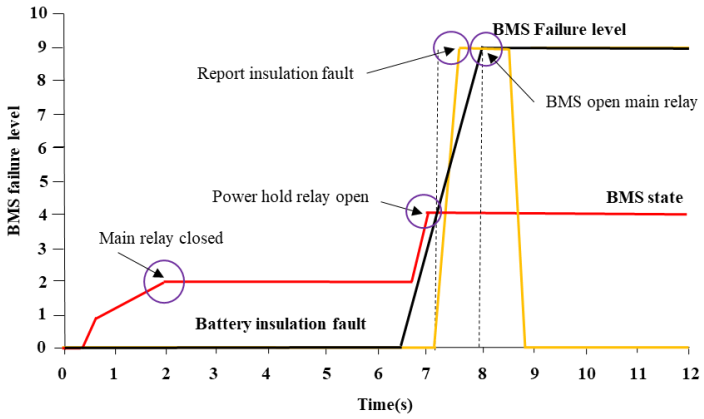


Fig. 8 Simulation result of battery insulation resistance based on fuzzy system

4.3 Identification and simulation of battery communication faults

Battery BMS communication failures are common, and while their consequences are typically not as severe as those of insulation failures, they still warrant attention. From a fault identification perspective, the abundance of signals available for cross-verifying communication faults indicates that the accuracy of diagnosing these faults should exceed that of insulation faults. In contrast, the limited signals available to validate insulation faults heighten the risk of misjudgment, making the identification of communication fault less challenging than that of insulation fault identification.

Should a loss of the CAN signal external to the BMS occur while driving, disrupting communication between the BMS and VCU, the BMS will typically be unable to process requests from the VCU. Under these circumstances, the BMS enters a limited power mode, capping both charging and discharging power at 10 kW, which causes the vehicle to enter a reduced operational state until it gradually comes to a halt. If an internal CAN signal loss within the BMS is detected during operation, signifying disrupted communication among BMS modules, a comprehensive evaluation is conducted using data on battery temperature, voltage, current, and internal resistance. If normal battery temperatures are observed alongside anomalies in voltage or current, this suggests

a malfunction in the BMS's internal CAN communication module, which poses minimal risk. The last received signal before the loss may serve as a temporary substitute to maintain BMS functionality. However, if temperature, voltage, and current signals are all absent, this indicates a fault in the BMS signal acquisition slave board, rendering battery data inaccessible and posing a significant risk of battery uncontrollability. In such cases, the battery must be deactivated, and a shutdown operation should be initiated.

Fig. 9 displays the simulation results of a fuzzy expert system designed for diagnosing battery communication faults. When the BMS detects a communication failure (indicated by the internal fault status changing from 0 to 1), it notifies the VCU of the internal communication issue. The VCU promptly updates the system fault level from 0 (no fault) to 1 (fault present). In response to the feedback regarding the internal fault status from the BMS and the system fault status from the VCU, the BMS also adjusts its fault level from 0 to 1. Throughout this process, the battery's minimum and maximum temperatures remain constant. Consequently, the power battery enters a power-limited mode, with the peak discharge power decreasing linearly from 240 kW to 10 kW at a rate of 20 kW/s, which takes approximately 11.5 seconds. Similarly, the continuous discharge power reduces from 240 kW to 10 kW, with a decline from 125 kW to 10 kW occurring at the same rate of 20 kW/s over approximately 5.75 seconds, in accordance with the design specifications.

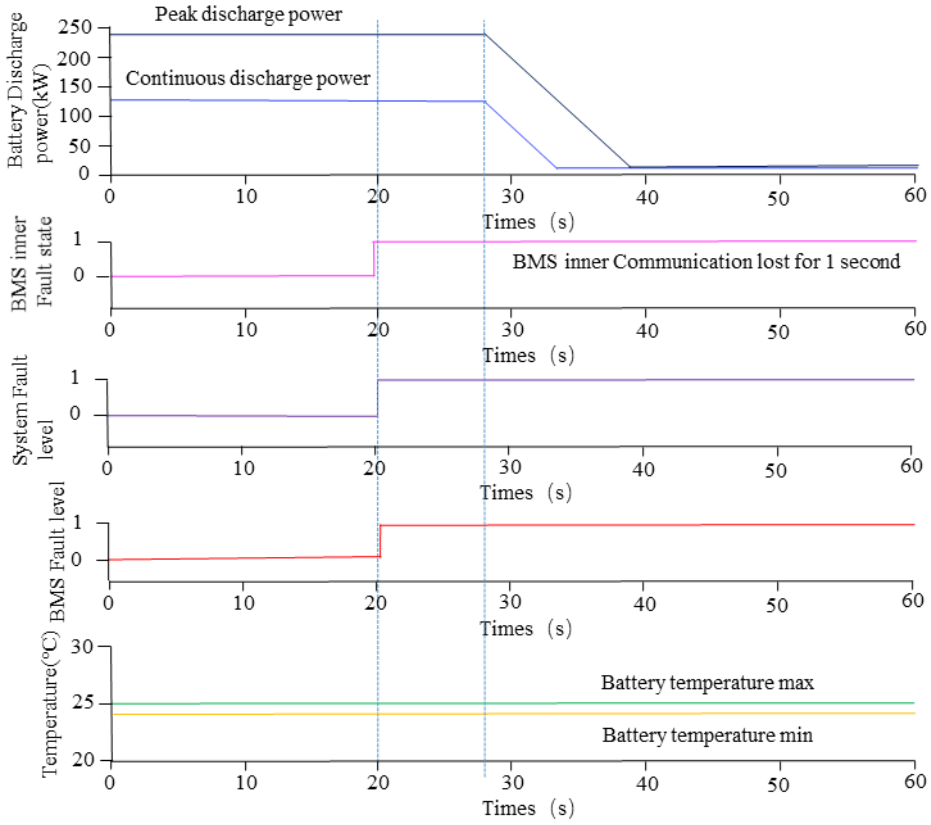


Fig. 9 Simulation result of battery communication based on fuzzy system

According to the BMS communication fault control threshold table and the corresponding handling measures shown in Tab. 2, it is evident that during the EV driving process, the communication fault diagnosis will only be initiated if the internal communication fault of the BMS persists for more than 2 second. A communication fault will only be confirmed if the communication signal is lost for 255 consecutive cycles. The communication cycle is 10 ms, while the communication signal transmission and recovery cycle is 20 ms. Therefore, the counting time for 255 communication cycles is approximately 5.1 seconds. It takes 2 communication cycles for the internal communication fault of the BMS to escalate to the fault level setting of the BMS. Consequently, the cumulative time for confirming the communication fault reaches 6.325 seconds. According to the BMS table lookup protocol, an additional 500 ms is required to complete the table lookup, during which the output charging and discharging power values are gradually reduced based on the principle of decrement. Therefore, it takes approximately 8.025 seconds for the peak and

continuous power of the power battery to gradually decrease. The simulation results presented in Fig. 9 meet the design expectations.

5. Discussion on experiment results

Insulation and communication fault tests were conducted using EVs. Various resistance values were introduced at different locations to simulate insulation faults, while communication faults were tested by deliberately disabling the communication function of the slave board through BMS software. Since the experimental results for insulation and communication faults are minimally influenced by temperature factors, this article focuses solely on experiments conducted in a normal temperature environment.

The experimental process evaluated under various environmental temperatures, operating conditions, and fault thresholds to ensure that the model maintained high accuracy and stability across different working conditions and input models. Subsequently, experiments were conducted on EV insulation faults and BMS communication faults under diverse operating conditions. Since these two types of faults are less sensitive to environmental temperature, there is no significant difference in the test results at varying temperatures. Therefore, this manuscript selected room temperature experimental data as a case study for illustration.

5.1 BMS insulation fault test



Fig. 10 BMS fault test and insulation fault test platform

Fig. 10 presents a schematic of the experimental setup, illustrating a test bench designed in accordance with the specified testing criteria. The top-left portion of the diagram showcases the HIL testing apparatus, which simulates various faults and communication signals within the power battery system. This equipment is utilized to evaluate the detection efficiency of the developed fuzzy judgment system. The experiment employed 100 test samples, a quantity nearly equivalent to the number of fault samples typically examined in real vehicles, making these results notably representative. The middle-top section of the figure depicts an experimental apparatus that replicates diverse input errors, communication signal discrepancies, and interference signals encountered by the BMS. This setup allows for the assessment of the BMS model's judgment accuracy through these simulated signals. In the bottom-left corner, the figure features a testing bench where actual signal measurement errors from the battery pack are introduced. This enables the examination and validation of the simulation system's fault diagnosis accuracy by integrating errors from various sensors. The right portion of Fig. 10 displays a device specifically designed for detecting insulation faults in actual vehicles. It introduces insulation resistance values at different levels to measure the accuracy of insulation fault detection.

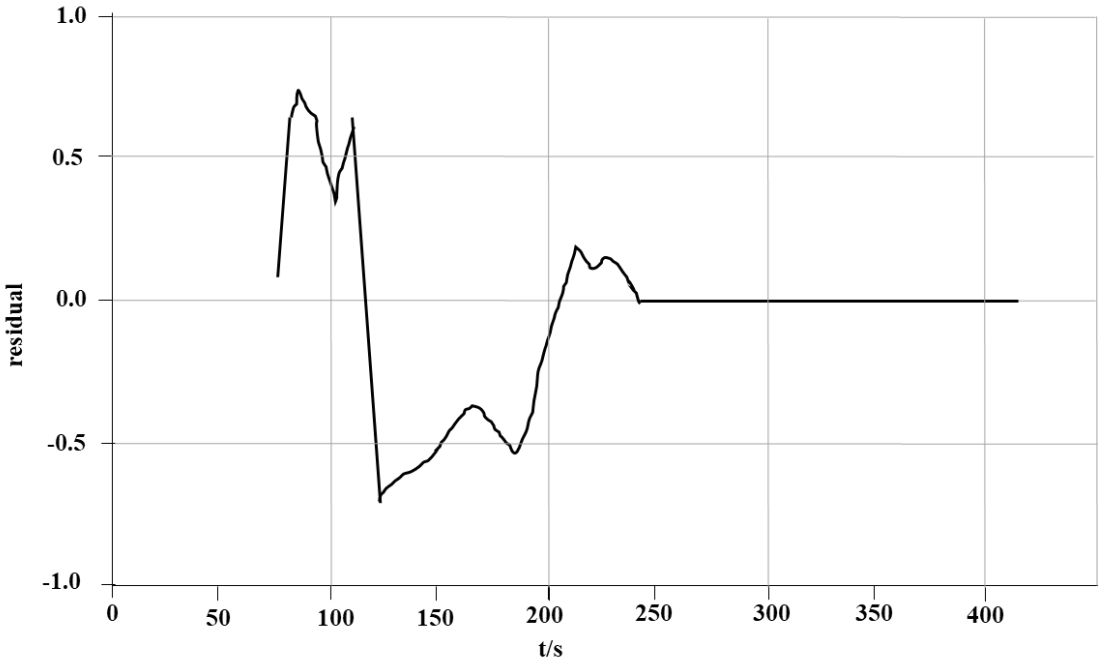


Fig. 11 Residual of insulation fault model based on fuzzy system

Fig. 11 illustrates the detection and analysis outcomes for insulation and overcurrent faults within the fault signals processed by the developed fuzzy system. During the initial 50 seconds, the system detects no faults. Following this period, both fault signals and interference signals are introduced, with insulation and overcurrent fault signals being input separately. As depicted in Fig. 8, during the fault-free initial 50 seconds, the fault model values closely align with the system's judgment values, indicating no discrepancies. However, upon the introduction of simulated fault and interference signals, a divergence between the system's judgment values and the input fault values emerges, leading to discrepancies. Despite this, the discrepancies remain minimal, all under 1.0. By the 220-second mark, the discrepancy value for insulation faults approaches 0, effectively eliminating inaccuracies in both the model and judgment values. Around the 330-second mark, the discrepancies related to overcurrent faults and judgment value inaccuracies essentially dissipate. Following thorough testing, the fuzzy recognition system demonstrates an effective capability to identify specific fault signal characteristics, with the model's judgment accuracy reaching approximately 92.7%, which is considered an outstanding achievement.

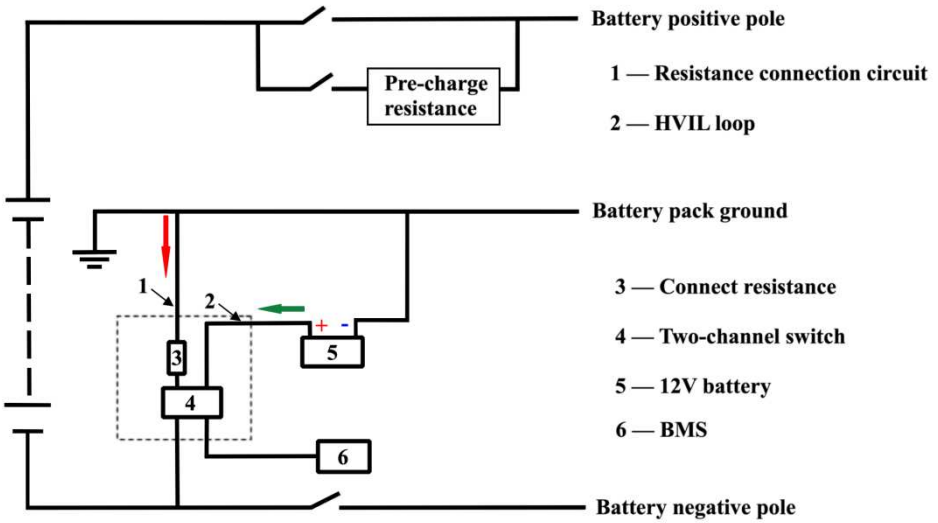


Fig. 12 Schematic diagram of insulation fault experiment for series resistance testing

Fig. 12 illustrates the layout of a test bench designed for identifying insulation faults in battery systems through a series resistance examination. In this configuration, a variable resistor (R) is connected in series between the main positive relay of the battery system and the ground. To measure the timing of insulation detection, a dual-channel switch, referred to as Switch 4, is integrated into both Circuit 1 and Circuit 2. Activating Switch 4 allows Circuit 1 to engage while Circuit 2 disengages. This arrangement enables the BMS to determine the precise moment when the insulation resistance connection begins by monitoring the status of Circuit 2.

The interval between the disconnection of the HVIL and the reporting of insulation faults is analyzed to determine the response time of the insulation detection system. The reported insulation resistance value is readily accessible, and the experimental findings are presented in Fig. 13.

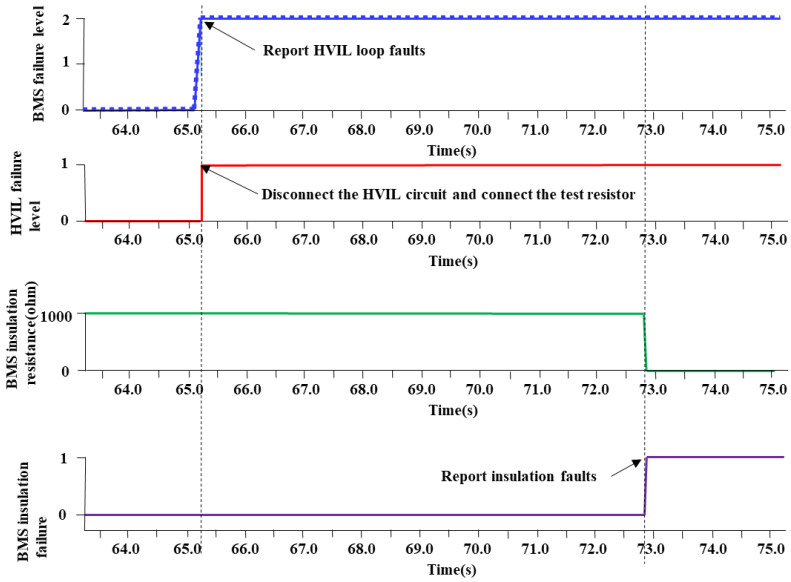


Fig. 13 Disconnect the HVIL circuit and connect the test resistor experiment while the vehicle is in operation

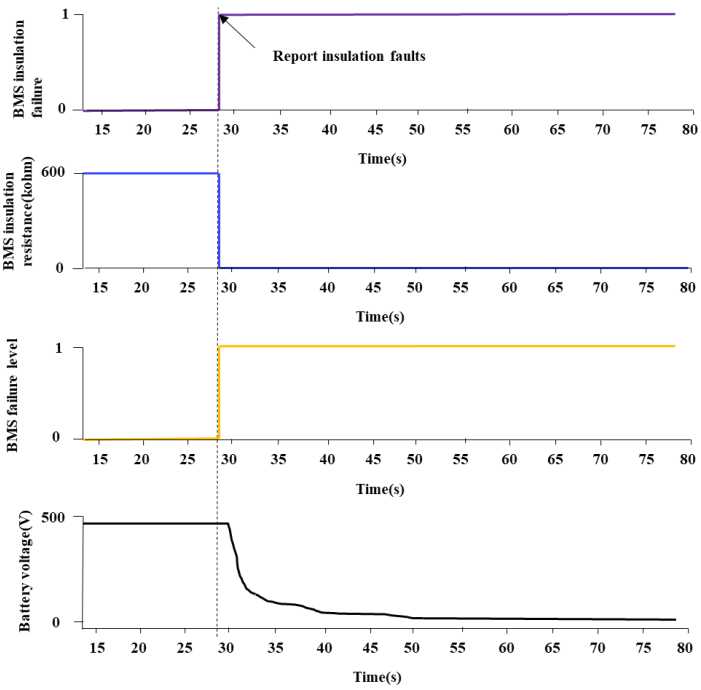


Fig. 14 Experimental results of battery insulation fault during positive pole grounding test inside battery pack during vehicle operation

Fig. 13 displays the results of tests conducted by grounding the positive pole of the battery pack and severing the HVIL circuit during standard vehicle operation. The findings indicate that upon disconnecting the HVIL circuit, the BMS promptly identifies an HVIL short circuit fault. At this point, the fuzzy judgment system performs a thorough assessment of the insulation detection results, integrating data from the insulation detection circuit and other sensor signals. After several iterations and validations, it takes approximately 7.6 seconds to confirm an insulation fault. Following this verification, the BMS immediately reports the fault. Although the fuzzy judgment system extends the duration of battery insulation detection, it significantly enhances detection accuracy. The experimental data confirm that the integration of a fuzzy fault judgment system substantially enhances the precision of insulation fault detection, with a slight increase in judgment duration deemed acceptable (the design criterion for insulation fault judgment duration is limited to 10 seconds).

Numerous experimental data have demonstrated that incorporating a fuzzy theory database for identifying battery insulation faults has enhanced the accuracy of fault detection from approximately 80% to 95%. This represents a significant enhancement. Although the detection time has increased from about 3 seconds to 7.6 seconds, it remains within the specified 10-second limit, making this a highly valuable outcome.

Fig. 14 elucidates that grounding the positive terminal of the battery pack during normal vehicle operation causes the insulation resistance recorded by the BMS to drop dramatically from 600 kΩ to 0 Ω, triggering an insulation fault alert from the BMS. This fault results in elevated voltage levels within the battery system. The test results show that disconnecting the main positive and negative relays of the battery pack activates the motor controller's rapid discharge circuit, which is connected to the external high-voltage circuit, leading to a rapid decrease in external high voltage. Within approximately 8 seconds, the voltage decreases to 0 V, meeting the design objective of reducing high voltage within 10 seconds. This outcome validates the effectiveness of the implemented battery fault diagnosis and remediation strategies.

5.2 BMS communication fault test

Fig. 15 outlines the outcomes of the BMS communication fault detection. The data presented in the figure illustrate a more rapid identification process for communication faults compared to insulation faults, with a significantly lower model residual for communication faults. The findings demonstrate that after more than 130 iterations, the fuzzy expert system accurately identifies communication faults, with the identified residual being markedly lower than that for insulation faults, thereby corroborating earlier analytical observations.

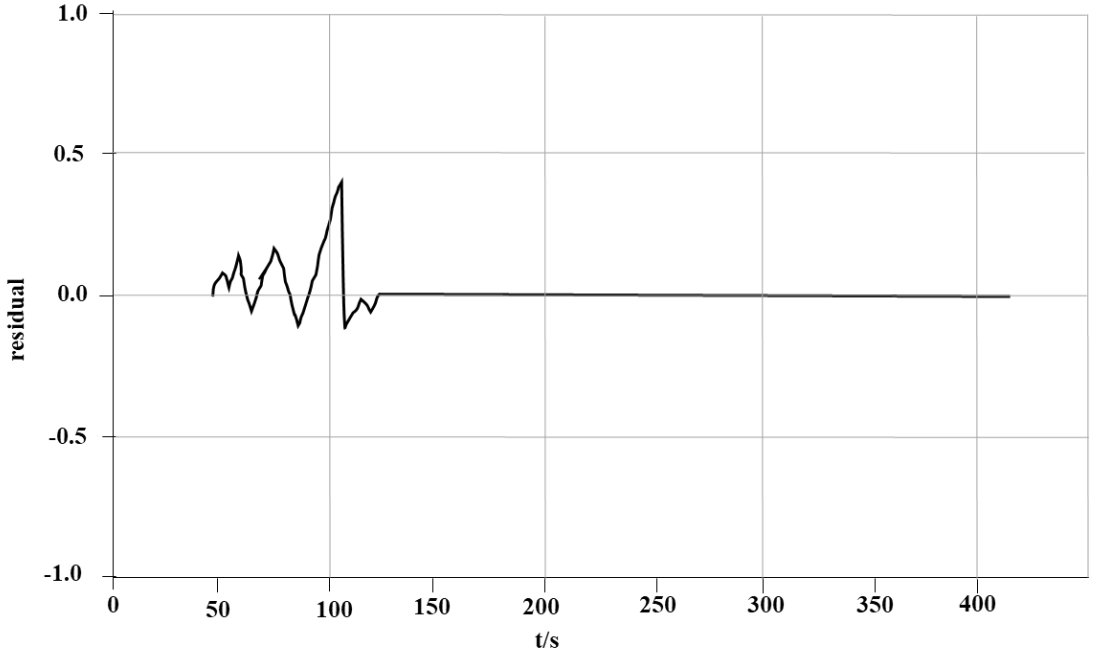


Fig. 15 Residual of communication fault model based on fuzzy system

Fig. 16 shows the experimental data regarding internal communication faults during EV operation. The results indicate that after the BMS reports an internal communication fault, the VCU categorizes the issue as a power reduction fault in the subsequent communication cycle. Meanwhile, the BMS must wait for a confirmation period of 2 seconds before reporting a BMS system fault. According to the simulation analysis presented in Figure 9, it takes approximately 8.2 seconds to initiate power reduction following the BMS's report of a system fault. It is important to note that actual driving conditions are likely to be more complex than those simulated. The fuzzy diagnosis system must integrate data from various sensors, model calculations of the power battery, and the power map of the BMS to accurately assess the reported peak and continuous power decline slope. This integration is crucial to ensure that the power of the EV does not experience sudden loss. During the confirmation process, the voltage, current, temperature, and communication signals of the power battery are in constant flux. The power reduction mode is not highly responsive to these power changes. Consequently, after repeated confirmations by the fuzzy diagnosis system, the peak power and continuous power begin to decrease after approximately 24 seconds, with the peak power dropping to 10 kW within about 20 seconds. As a result, EV exhibits insufficient power and reduced acceleration, which aligns with the design expectations.

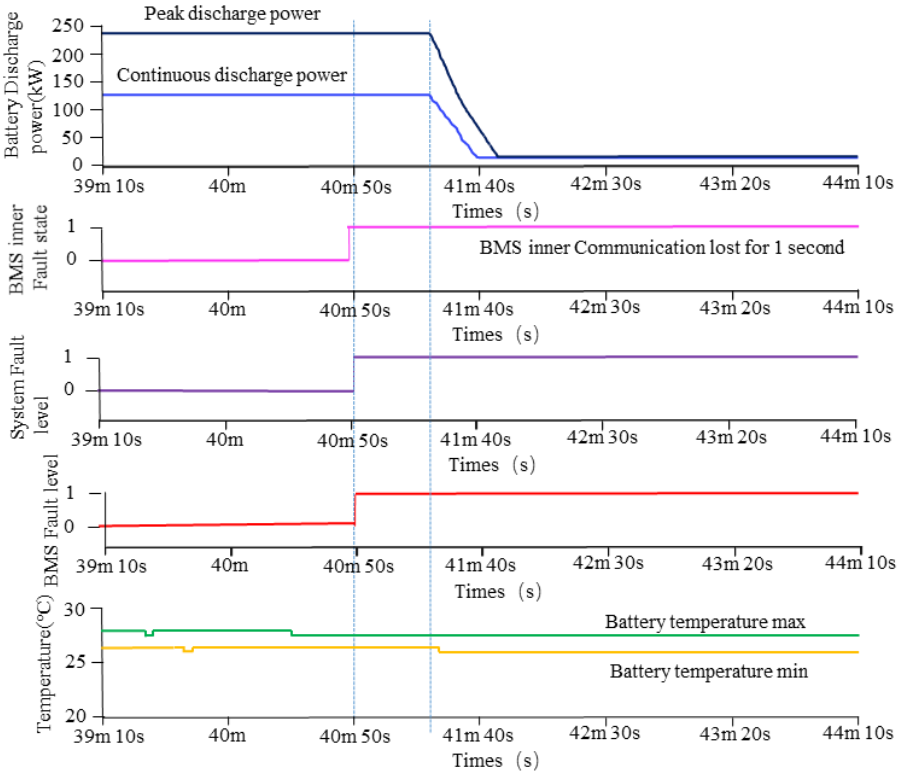


Fig. 16 Experimental results of battery communication fault during vehicle driving

Fuzzy theory can improve the accuracy of fault diagnosis battery sector; however, it also increases the time required for fault diagnosis. While it currently has a significant impact on diagnosing power battery faults, this remains a challenge that needs further resolution. The next phase of this study will focus on investigating how fuzzy theory can improve the accuracy and robustness of fault diagnosis systems. Additionally, a comparison will be made between the advantages and disadvantages of deep learning algorithms and those of fuzzy theory fault diagnosis algorithms.

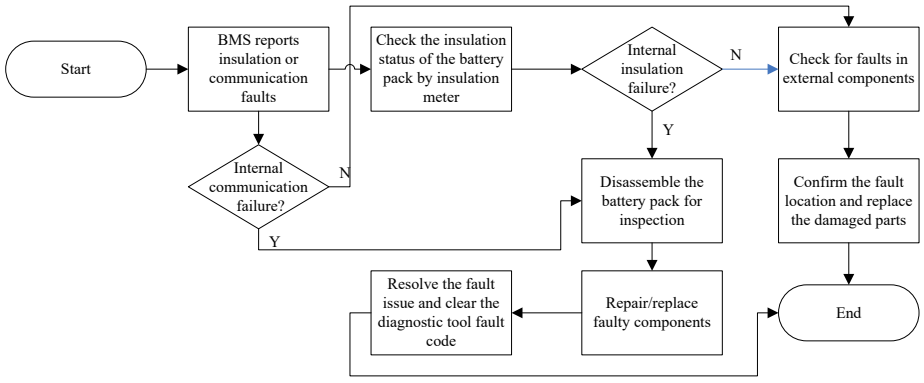


Fig. 17 Fault handling flowchart

Fig. 17 illustrates the flowchart for fault handling. Upon detecting battery insulation or communication faults, the process proceeds as outlined in Fig 17. The BMS determines whether the fault is an internal or external insulation fault of the battery pack, or an internal or external communication fault. For insulation faults, an insulation meter is used for actual measurement and troubleshooting. If the fault is identified as being within the battery pack, the pack should be disassembled to locate the fault. Once the fault location is confirmed, any damaged components

should be repaired or replaced. Conversely, if the fault is external to the battery pack, the faulty components in the high-voltage circuit outside the pack should be checked sequentially. After confirming the fault, the damaged components must also be repaired or replaced. Once repairs are completed and the fault has been verified as resolved, the historical fault records stored in the BMS memory should be cleared, and the diagnostic instrument fault codes should be reset to conclude the fault diagnosis process.

In summary, combining experimental data with utilizing fuzzy theory to construct and adjust a fuzzy expert database and fuzzy relationships for battery calculation models can improve the accuracy and robustness of battery fault diagnosis. Both simulated and empirical data demonstrate that the fuzzy theoretical model developed for diagnosing battery system faults exhibits high accuracy in fault detection. Although the judgment time is slightly extended, it remains within the acceptable limits of the design specifications. The findings of this study offer considerable insights and serve as a valuable reference for similar research endeavors in the field. Results from multiple repeated experiments indicate that the judgment time of the designed BMS fuzzy diagnosis system has increased by approximately 4.6 seconds; however the accuracy of insulation fault diagnosis has improved from 81.1% to 92.3%, and the true accuracy of communication fault diagnosis has risen from 91.4% to 97.7%, reflecting a significant improvement. Compared to similar studies, the accuracy of BMS fault diagnosis is notably high, and the measures implemented after fault confirmation also ensure the safety of drivers and passengers.

6. Conclusions

This paper integrates fuzzy theory into the development of fault diagnosis systems for power battery systems, focusing on the detection of unpredictable battery faults under various operational conditions and confirming the presence of actual faults. While prioritizing identification accuracy, the study also aims to enhance the iteration count to further refine fault identification precision.

The findings of this paper primarily include:

A fault diagnosis system for power batteries is developed using fuzzy theory. The design includes the judgment principles, thresholds, and methods for handling fault. Additionally, simulation analysis and experimental verification are conducted for two typical faults in the power battery system: insulation faults and communication faults.

The simulation results and experimental verification outcomes of the developed fuzzy fault diagnosis system align with the design requirements, demonstrating a close correlation. This indicates that the designed fuzzy fault diagnosis system exhibits strong robustness and accuracy.

Compared to the research findings of other peers both domestically and internationally, the BMS fuzzy fault diagnosis system developed in this article increases the fault diagnosis judgment by approximately 6 seconds. However, it significantly improves the accuracy of diagnosing insulation and communication faults.

Improving the efficiency of battery fault diagnosis and assessment is crucial. GPU or FPGA chips can enhance computing speed, they are often prohibitively expensive. Consequently, the next area of research will focus on how to balance design requirements with cost consideration. At present, GPU chip solutions are not viable due to their high production costs.

During the battery fault diagnosis process, this paper introduces fuzzy theory to develop a fuzzy database, aiming to enhance both the accuracy and judgment speed of battery fault diagnosis. In the future, big data analysis technology will increasingly be applied in the field of power battery fault diagnosis. The integration of power batteries with big data represents a significant trend in the evolving industry. By leveraging the massive data generated during the operation of electric vehicles, establishing a battery system fault diagnosis and prediction system from the perspective of big data analysis has become a key focus and research hotspot. Moreover, machine learning algorithms have proven their effectiveness and reliability in constructing power battery fault prediction models. In the coming years, the incorporation of more advanced network learning algorithms in the battery fault diagnosis field is an inevitable trend.

Acknowledgement

The authors would like to thank the support from the Guangdong Provincial Natural Science Foundation Project (2020A1515010382).

Data Availability Statement

The datasets used and/or analysed during the current study available from the corresponding author on reasonable request.

References

[1] Xiong, R.; Sun, W.; Yu, Q.; Sun, F. Research progress, challenges and prospects of fault diagnosis on battery system of electric vehicles. *Appl. Energy* ***2020****, 279,* 115855.

[2] Zhao, J.; Feng, X.; Tran M.; Fowler, M.; Ouyang, M.; Burke A.F. Battery safety Fault diagnosis from laboratory to real world. *J. Power Sources* ***2024****, 598,* 234111.

[3] Tian, J.; Yin, J.; Insulation fault monitoring of lithium-ion battery pack: Recursive least square with adaptive forgetting factor. *J. Energy Storage* ***2023****, 67,* 107624.

[4] Wang, Y.; Tian, J.; Chen, Z.; Liu, X. Model based insulation fault diagnosis for lithium-ion battery pack in electric vehicles. *Measurement* ***2019****, 131,* 443-451.

[5] Tian, J.; Wang, Y.; Yang, D.; Zhang, X.; Chen, Z. A real-time insulation detection method for battery packs used in electric vehicles. *J. Power Sources* ***2018****, 385,* 1-9.

[6] Song, C.; Shao, Y.; Song, S.; Peng, S.; Zhou, F.; Chang, C.; Wang, D. Insulation Resistance Monitoring Algorithm for Battery Pack in Electric Vehicle Based on Extended Kalman Filtering. *Energies* ***2017****, 10,* 714.

[7] Hu, L.; Hu, X.; Che, Y.; Feng, F.; Lin, X.; Zhang, Z. Reliable state of charge estimation of battery packs using fuzzy adaptive federated filtering. *Appl. Energy* ***2020****, 262,* 114569.

[8] Wang, G.; Jin, B.; Wang, M.; Sun, Y.; Zheng, Y.; Su, T. State of charge estimation for "$LiFePO_4$ - $LiCo_xNi_yMn_{1-x-y}O_2$" hybrid battery pack. *J. Energy Storage* ***2023****, 65,* 107345.

[9] Zhao, J.; Feng, X.; Tran, M.-K.; Fowler, M. Ouyang, M. Battery safety: Fault diagnosis from laboratory to real world. *J. Power Sources* ***2024****, 598,* 234111.

[10] Liu, Q.; Ma, J.; Zhao, X.; et al. Voltage fault diagnosis and misdiagnosis analysis of battery systems using the modified Shannon entropy in real-world electric vehicles. *J. Energy Storage* ***2023,*** *73,* 109287.

[11] Zhang, X.; Hong, J.; Xu, X. Fault diagnosis of real-scenario battery systems based on modified entropy algorithms in electric vehicles. *J. Energy Storage* ***2023****, 63,* 107079.

[12] Kang, Y.; Duan, B.; Zhou, Z.; Shang, Y.; Zhang, C. A multi-fault diagnostic method based on an interleaved voltage measurement topology for series connected battery packs. *J. Power Sources* ***2019****, 417,* 132-44.

[13] Hong, J.; Wang, Z.; Wen, C.; et al. Online joint-prediction of multi-forward-step battery SOC using LSTM neural networks and multiple linear regression for real-world electric vehicles. *J. Energy Storage* ***2020****, 30,* 101459.

[14] Li, K.; Zhou, P.; Han, X.; Li, X.; Zheng, Y. Battery life estimation based on cloud data for electric vehicles. *J. Power Sources* ***2020****, 468,* 228192.

[15] Ouyang, N.; Zhang, W.; Yin, X.; Li, X.; Xie, Y.; He, H.; A data-driven method for predicting thermal runaway propagation of battery modules considering uncertain conditions. *Energy* ***2023,*** *273,* 127168.

[16] Jiang, L.; Deng Z.; Tang, X.; et al. Data-driven fault diagnosis and thermal runaway warning for battery packs using real-world vehicle data. *Energy* ***2021****, 234,* 121266.

[17] Machlev, R. EV battery fault diagnostics and prognostics using deep learning: Review, challenges & opportunities. *J. Energy Storage* ***2024****, 83,* 110614.

[18] Lee, H. J.; Kim, K. T.; Park, J. H.; Bere, G.; Ochoa, J. J.; Kim, T. Convolutional neural network-based false battery data detection and classification for battery energy storage systems. *IEEE Trans. Energy Convers.* ***2021****, 36 (4),* 3108-3117.

[19] Kosuru, V.S.R.; Venkitaraman, A. K. A smart battery management system for electric vehicles using deep learning-based sensor fault detection. *World Electr. Veh. J.* ***2023,*** *14 (4),* 101.

[20] Wassiliadis, N.; Steinstrater, M.; Schreiber, M.; et al. Quantifying the state of the art of electric powertrains in battery electric vehicles Range, efficiency, and lifetime from component to system level of the Volkswagen ID.3. *eTransportation* ***2022****, 12,* 100167.

[21] Mousa, A.R.; ElSayed, M.S.; Jurcut, A.; Azer, M.A. lightweight-X-authentication protocol over automotive gateway. *Comput. Electr. Eng.* ***2023****, 110,* 108887.
[22] Buquerin, K.K.G.; Corbett C.; Hof H. A generalized approach to automotive forensics. *Forens. Sci. Int-Digit* ***2021****, 36,* 301111.
[23] Nasser, A.M.K.; Ma, D. SecMonQ: An HSM based security monitoring approach for protecting AUTOSAR safety-critical systems. *Veh. Commun.* ***2020****, 21,* 100201.
[24] Dobromirov, V.; Dotsenko, S.; Verstov, V.; Volkov S. Methods of Examining Vehicle Electronic Systems in the Course of Automotive Forensic Expert Examinations. *Transportation Research Procedia* ***2017****, 20,* 143-150.
[25] Zhang, J.; Rizzoni, G. Functional Safety of Electrified Vehicles Through Model-Based Fault Diagnosis. *IFAC-PapersOnLine* ***2015****, 48-15,* 454-461.
[26] Tian, J.; Liu, X.; Chen, C.; et al. Feature fusion-based inconsistency evaluation for battery pack: improved gaussian mixture model. *IEEE Trans. Intell. Transp. Syst.* ***2022****, 24,* 446-458.
[27] Tang, A.; Huang, Y.; Liu, S.; Yu, Q.; Shen W.; Xiong, R. A novel lithium-ion battery state of charge estimation method based on the fusion of neural network and equivalent circuit models. *Appl. Energy* ***2023****, 348,* 121578.
[28] Xiong, R.; Cao, J.; Yu, Q.; He, H.; Sun, F. Critical Review on the Battery State of Charge Estimation Methods for Electric Vehicles. *IEEE Access,* ***2017****, 6,* 1832-1843.
[29] Chen, Z.; Zhao, H.; Shu, X.; Zhang, Y.; Shen, J.; Liu, Y. Synthetic state of charge estimation for lithium-ion batteries based on long short-term memory network modeling and adaptive H-Infinity filter. *Energy* ***2021****, 228,* 120630.
[30] Zhang, Z.; Jiang, L.; Zhang, L.; Huang, C. State-of-charge estimation of lithium-ion battery pack by using an adaptive extended Kalman filter for electric vehicles. *J. Energy Storage* ***2021****, 37,* 102457.
[31] Ren, S.; Sun, J. Multi-fault diagnosis strategy based on a non-redundant interleaved measurement circuit and improved fuzzy entropy for the battery system. *Energy* ***2024****, 292,* 130603.
[32] Kim, E.; Oh, S.; Pedrycz, W. Reinforced hybrid interval fuzzy neural networks architecture: Design and analysis. *Neurocomputing* ***2018****, 303,* 20-36.
[33] Mendes, J.; Araujo, R.; Matias, T.; Seco, R.; Belchior, C. Automatic extraction of the fuzzy control system by a hierarchical genetic algorithm. *Eng. Appl. Artif. Intel.* ***2014****, 29,* 70-78.
[34] Bicen, Y.; Aras, F.; Smart asset management system for power transformers coupled with online and offline monitoring technologies. *Eng. Fail. Anal.* ***2023****, 154,* 107674. [CrossRef]
[35] Alshomrani, S.; Bawakid, A.; Shim, S.; Fernandez, A.; Herrera, F. A proposal for evolutionary fuzzy systems using feature weighting: Dealing with overlapping in imbalanced datasets. *Knowl-Based Syst.* ***2015****, 73,* 1-17.
[36] Nan, C.; Khan, F.; Iqbal, M.T. Real-time fault diagnosis using knowledge-based expert system. *Process Saf. Environ.* ***2008****, 86,* 55-71.
[37] Jan, S.U.; Lee, Y.D.; Koo, I.S. A distributed sensor-fault detection and diagnosis framework using machine learning. *Inform. Sciences* ***2021****, 547,* 777-796.
[38] Rozas, H.; Claveria, R.M.; Orchard, M.E.; Medjaher, K. Residual-based scheme for detection and characterization of faults in lithium-ion batteries. *IFAC PapersOnLine* ***2018****, 51-24,* 200-207.